



Review

# Beyond Ultrasound: Multimodal Cross-Sectional Imaging for Preoperative Imaging of Parotid Gland Tumors: A Primer for Radiology Trainees

Esmat Mahmoud <sup>1</sup>, Eman Mahdi <sup>2</sup> , Humera Ahsan <sup>3</sup>, Joseph P. Cousins <sup>3</sup>, Carlos Leiva-Salinas <sup>3</sup> and Ayman Nada <sup>3,\*</sup>

<sup>1</sup> Department of Diagnostic and Interventional Radiology, National Cancer Institute, Cairo University, Cairo 11796, Egypt; esmat3m@gmail.com

<sup>2</sup> Department of Radiology, Virginia Commonwealth University, Richmond, VA 23284, USA; eman.mahdi@vcuhealth.org

<sup>3</sup> Department of Radiology, University of Missouri, Columbia, MO 65211, USA; ahsanh@health.missouri.edu (H.A.); cousinsj@health.missouri.edu (J.P.C.); salinascl@health.missouri.edu (C.L.-S.)

\* Correspondence: anada@health.missouri.edu

**Abstract:** Even if the management of parotid gland tumors depends on the histopathological subtype, preoperative imaging of parotid gland tumors is clinically relevant. Preoperative imaging gives insight into the differentiation between benign and malignant tumors, which might potentially decrease the number of unnecessary aggressive surgeries. Characteristic imaging findings on cross-sectional imaging, such as computed tomography (CT) and magnetic resonance imaging (MRI), can help narrow the differential diagnosis and guide the further management of patients presenting with parotid masses. While MRI is imperative for the determination of perineural spread, which is frequently encountered with malignant parotid tumors, CT is important for the evaluation of osseous invasion. Furthermore, multi-parametric MRI protocols provide insights into the tumor behavior and internal composition, which is helpful in the case of benign mixed tumors and others. While distant metastasis is uncommon with parotid neoplasms, PET/CT provides a valuable tool for the improved evaluation of loco-regional and distant metastatic disease. This article discusses the imaging features of common benign and malignant parotid tumors.

**Keywords:** parotid gland tumors; benign and malignant tumors; CT; MRI; PET/CT



**Citation:** Mahmoud, E.; Mahdi, E.; Ahsan, H.; Cousins, J.P.; Leiva-Salinas, C.; Nada, A. Beyond Ultrasound: Multimodal Cross-Sectional Imaging for Preoperative Imaging of Parotid Gland Tumors: A Primer for Radiology Trainees. *J. Otorhinolaryngol. Hear. Balance Med.* **2024**, *5*, 1. <https://doi.org/10.3390/ohbm5010001>

Academic Editor: Norihiko Narita

Received: 6 December 2023

Revised: 17 January 2024

Accepted: 18 January 2024

Published: 23 January 2024



**Copyright:** © 2024 by the authors. Licensee MDPI, Basel, Switzerland. This article is an open access article distributed under the terms and conditions of the Creative Commons Attribution (CC BY) license (<https://creativecommons.org/licenses/by/4.0/>).

## 1. Introduction

Most salivary gland neoplasms develop within the parotid glands [1]. Generally, ~70–85% are benign, while the rest are malignant [2]. The surgical management of parotid gland tumors differs greatly for benign and malignant neoplasms [3]. While the former are treated with extracapsular dissection or superficial parotidectomy, the latter need more aggressive surgical approaches, such as total parotidectomy and neck dissection with potential adjuvant therapy [3].

The classic presentation of a slowly growing painless preauricular swelling or mass is not conclusive for either benign or malignant parotid gland neoplasms. Facial nerve palsy is probably the most robust clinical symptom suggesting malignancy [4]. Therefore, preoperative imaging is critical in surgical planning to assess tumor extension and evaluate imaging criteria that might predict malignancy [5]. Such information helps surgeons to determine the most appropriate therapeutic procedure and surgical approach.

Cross-sectional imaging modalities such as ultrasound, CT, MRI, and PET/CT are helpful for the imaging work-up for the evaluation of patients presenting with parotid masses. Given its feasibility, lack of radiation exposure, and the superficial position of

the parotid glands, ultrasound is the first-choice imaging modality for the evaluation of mass morphology including borders and margins [1,2]. Benign masses are typically well defined with smooth margins and regular borders, while malignant masses are typically ill defined with irregular borders. The identification of the external carotid artery and retromandibular vein at the posterior mandibular angle represents a line of demarcation between the superficial and deep lobes of the parotid glands. Ultrasound is sufficient for the evaluation of masses within the superficial lobe of the parotid gland, yet masses within the deep lobe or with aggressive features such as osseous invasion or perineural spread will require further evaluation with CT or MRI for better assessment [1,4–6].

In the current article, we review the imaging features of the most common parotid tumors using cross-sectional imaging with computed tomography (CT), magnetic resonance (MR) imaging, and fluorodeoxyglucose (FDG)-positron emission tomography (PET)/CT. Though ultrasound is the initial imaging modality for the evaluation of parotid masses, ultrasound imaging characteristics of parotid tumors are beyond the scope of this review. The distinction between benign and malignant parotid tumors based on imaging features is not always obvious, given the substantial overlap in imaging appearances. Nonetheless, it is useful for radiologists to be familiar with the various pathologies and typical imaging features of each type to decrease the rate of unnecessary aggressive interventions.

## 2. Benign Parotid Gland Tumors

Benign parotid gland tumors encompass a wide histopathological variability with several tumor-like conditions [3]. The most common imaging characteristics are well-defined masses with sharp margins, a hypointense rim on T2 WIs, and a lack of invasion of the surrounding structures or perineural extension on CT and MRI [6]. Advanced MRI techniques can help to differentiate benign from malignant parotid neoplasms (Figure 1) [7]. Previous studies found a potential role of diffusion-weighted imaging and diffusion tensor imaging with cutoff values in differentiating benign and malignant parotid tumors for ADC and fraction anisotropy (FA) of  $1.02 \times 10^{-3} \text{ mm}^2/\text{s}$  and 0.24, respectively [7]. We will focus on the commonly encountered parotid gland tumors, as shown in Table 1.

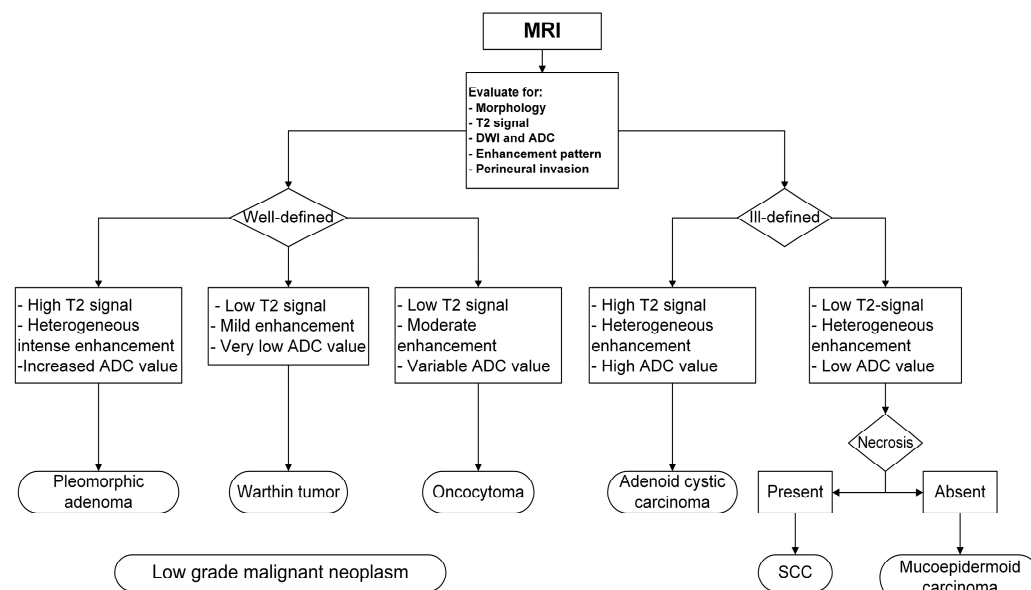


**Figure 1.** Suggested practical MRI approach to narrow differential diagnosis of parotid masses. ADC: apparent diffusion coefficient; DWI: diffusion-weighted imaging; MRI: magnetic resonance imaging; SCC: squamous cell carcinoma.

**Table 1.** Typical imaging features of common benign and malignant parotid tumors.

	Morphology	Margins	Composition	CT Enhancement	MRI Signal				Other Features
					T1	T2	DWI	Enhancement	
<b>Pleomorphic adenoma</b>	Well defined	Lobulated	Solid	Heterogeneous	Low	High	High ADC	Heterogeneous	
<b>Warthin tumor</b>	Well circumscribed	Regular	Solid, cystic-solid	Heterogeneous	Low	Low	Low ADC	Mild homogenous	Multiple, bilateral
<b>Oncocytoma</b>	Well defined	Usually lobulated	Predominantly solid	Mildly homogenous	Intermediate	Intermediate	High ADC	Mild homogenous enhancement	Vanishing tumor Non-enhancing curvilinear cleft
<b>Mucoepidermoid carcinoma</b> <b>Low-grade</b> <b>High-grade</b>	Well circumscribed	Micro-lobulated	Solid	Usually homogenous	Low	High	Usually homogenous		Perineural invasion
	Ill defined	Irregular	Solid	Heterogeneous	Intermediate-low	Intermediate-low	Low ADC	Heterogeneous	
<b>Adenoid cystic carcinoma</b>	Well defined	Smooth	Solid and cystic	Heterogeneous	Low	High	High ADC	Heterogeneous	Perineural invasion
<b>Acinic cell carcinoma</b>	Ill defined	Irregular	Solid		Low	Low	Low ADC	Heterogeneous	Perineural invasion
<b>Squamous cell carcinoma</b>	Ill defined	Irregular	Necrotic	Heterogeneous rim enhancing	Low	High	Low ADC	Heterogeneous peripheral enhancement	Perineural invasion
<b>Lymphoma</b>	Well circumscribed	Regular	Usually solid	Homogenous	Low	Low-intermediate	Low ADC	Homogenous	

ADC: apparent diffusion coefficient; DWI: diffusion-weighted imaging; MRI: magnetic resonance imaging.

## 2.1. Pleomorphic Adenoma

Pleomorphic adenomas (PAs) represent the most common benign salivary gland neoplasms, accounting for 50–75% of all salivary gland neoplasms as well as 70–80% of benign tumors [8]. Due to the variable contents within their matrix, they are also referred to benign mixed tumors of salivary glands. They are particularly prevalent in the parotid gland [9]. PAs are most frequently observed in the 3rd–6th decades, with a slightly higher incidence in females than in males [10].

The CT and MRI features of PAs depend on their size (Figure 2). Small tumors tend to be well defined, with multilobulated or bosselated margins and a homogeneously hyperintense signal on T2 WIs and a hypointense signal on T1 WIs relative to the muscles of mastication. They also exhibit solid intense enhancement after contrast administration [1]. On occasions, they might show a thin rim of T2 hypointensity representing a fibrous capsule. Larger tumors tend to show exophytic outgrowth with a heterogeneous signal and enhancement due to internal necrosis and hemorrhagic changes [11]. PAs usually have increased diffusivity with high ADC values due to their high content of chondroid and myxoid matrix (Figure 2) [12–14]. The range of ADC values of PAs varies among different studies ( $1.5\text{--}2.2 \times 10^{-3} \text{ mm}^2/\text{s}$ ) [7].

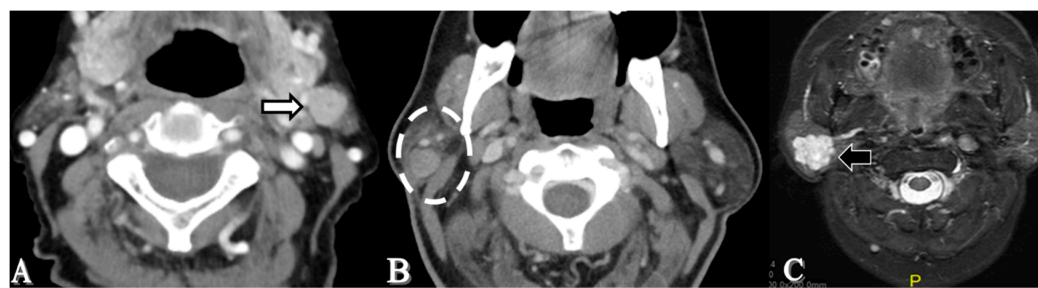


**Figure 2.** Parotid pleomorphic adenoma in 3 different patients. Axial contrast-enhanced CT image (A) of a left parotid PA in a 90-year-old female shows a small, well-circumscribed enhancing mass within the anteromedial portion of the left parotid tail (arrow). Axial contrast-enhanced CT image (B) of a right parotid PA in a 69-year-old female shows a small, well-circumscribed ovoid-shaped enhancing mass within the posteromedial portion of the right parotid tail (dashed circle). Axial Short Tau Inversion Recovery (STIR) image (C) of a right parotid PA in a 69-year-old female shows a well-circumscribed lobulated mass within the deep lobe of the right parotid gland. The mass has characteristic T2 hyperintensity (arrows). The left lateral retropharyngeal lymph node is partially imaged.

The most concerning prognostic consideration with PA is potential post-surgical recurrence, which has been reported to vary between 1% and 50% [15]. This variation depends upon the initial surgical approach [16]. PAs have the potential for malignant transformation into malignant mixed tumor (carcinosarcoma) (Figure 3) and carcinoma ex-pleomorphic adenoma [17]. Metastasizing pleomorphic adenoma is histologically benign, similar to pleomorphic adenoma, with local or distant metastatic lesions, particularly following multiple reoperations [16,17].

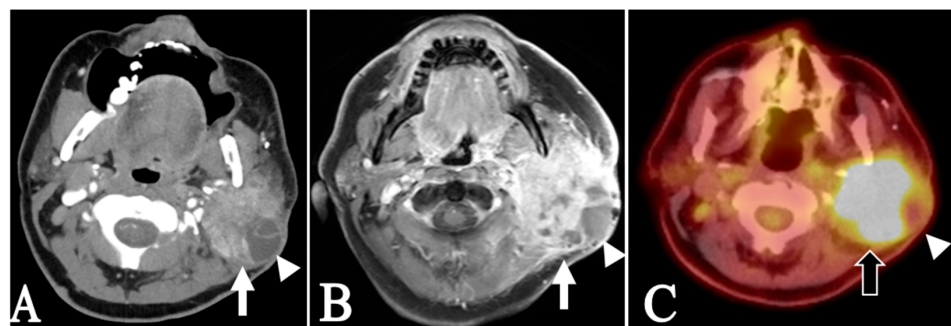


**Figure 3.** Left parotid, radiation-induced carcinosarcoma in a 51-year-old male. Axial contrast-enhanced CT image (A) shows a large heterogeneously enhancing mass involving the left parotid gland (white arrow), with internal areas of necrosis (arrowhead). Axial fat-saturated contrast-enhanced T1 image (B) shows a heterogeneously enhancing mass within the left parotid gland (arrows), with areas of necrosis at the posterolateral margins of the lesion (arrowhead). Axial FDG-PET/CT image (C) demonstrates avid FDG uptake of the enhancing solid components of the mass (wide arrow). The area of necrosis lacks FDG uptake (arrowhead).

## 2.2. Warthin Tumor

Warthin tumors (WTs) are the second most common benign parotid gland tumors in adults [18], accounting for 4–25% of all salivary gland tumors. The tail of the parotid gland is the most common location [19]. WTs typically contain dense lymphoid parenchyma; therefore, they are also known as papillary cystadenoma lymphomatosum or adenolymphoma [18]. WTs are the most common parotid tumor to present as multifocal bilateral nodules, which occurs in up to 10% of cases [17]. They often appear as a slowly progressive parotid gland swelling in older male subjects (typically >60 years) [20–22].

WTs present as well-circumscribed mixed cystic and solid mass lesions on CT (Figure 4) or MRI [1,23]. On T2 WIs, the solid components of WTs have a hypointense signal with a relatively poor contrast enhancement on post-contrast series (Figure 4) [23]. This helps to differentiate WT from PA. WTs also have restricted diffusivity with low ADC values due to the propensity of internal lymphoid tissue. This tumor is to be considered in the differential diagnosis of multifocal parotid masses, along with metastases, metastatic intra-parotid lymph nodes, lymphoma, benign lymphoepithelial lesions, and other inflammatory disorders (Figure 4) [3].

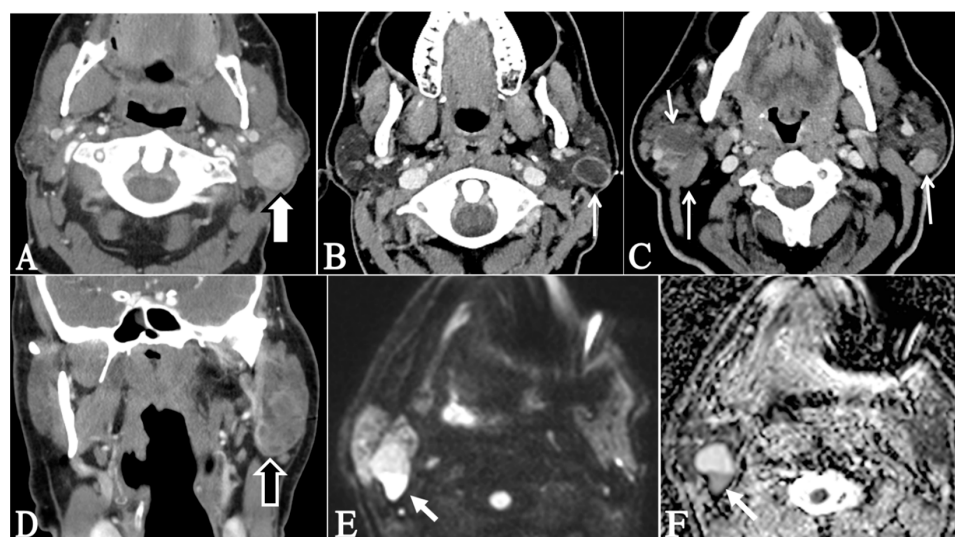


**Figure 4.** Variable imaging presentations of Warthin tumors. Axial contrast-enhanced CT image (A) of left parotid WT in a 59-year-old male reveals a well-circumscribed ovoid-shaped heterogeneously

enhancing mass within the posterior margin of the superficial lobe of the left parotid gland (arrows). The mass indents the underlying left sternomastoid muscle with a clear line of cleavage. Axial contrast-enhanced CT image (B) of a left parotid WT in a 32-year-old male shows a well-circumscribed rim-enhancing mass within the posterior margin of the superficial lobe of the left parotid gland (arrow). The mass is partly exophytic and abuts the overlying skin. Axial contrast-enhanced CT image (C) of bilateral parotid WTs in a 60-year-old male demonstrates multifocal well-circumscribed mildly enhancing masses within the parotid glands bilaterally (long arrows). The mass within the right deep parotid lobe appears hypodense with peripheral enhancement (short arrow). Coronal contrast-enhanced CT image (D) of a left parotid WT in a 62-year-old male demonstrate a well-circumscribed multi-loculated peripherally enhancing mass within the postero-inferior margin of the left parotid gland (wide arrow). Diffusion-weighted image (E) and corresponding ADC map (F) of a right parotid WT in a 64-year-old male demonstrate restricted diffusivity within the small enhancing focus within the posteromedial margin of the mass (arrows).

### 2.3. Lipoma

Parotid gland lipoma is uncommon and accounts for 0.6–4.4% of parotid lesions [24,25]. Lipomas appear as oval-shaped well-circumscribed masses within the parotid gland. Lipomas are characterized by their fat content, being easily recognized on CT and MRI, secondary to the typical hypodense CT attenuation values (generally HU –50 to –150) and fat signal intensities on all MR pulse sequences [26].

### 2.4. Oncocytoma

Oncocytomas represent benign epithelial parotid gland tumors that most frequently occur between the sixth and eighth decades of life with a slight female predominance [27]. Oncocytomas are rare and account for only 1% of all salivary gland tumors [28–31].

Parotid oncocytomas appear as well-defined sharply marginated masses on CT with non-enhancing clefts, as suggested by Tan et al. (Figure 5) [1,29]. Large oncocytomas are deformable and distorted when extended into the stylomandibular groove [29]. They have been called vanishing parotid tumors as they appear iso-intense to adjacent normal parotid glands in MRI [30]. Oncocytomas share imaging characteristics with WTs, and both have an iso- to hypointense signal on T2 WIs [32]. In addition, both demonstrate avid FDG activity on PET/CT and accumulate  $Tc^{99m}$  pertechnetate, possibly due to their high content of metabolically active mitochondria [30]. While oncocytomas appear hyperintense on fat-saturated contrast-enhanced T1 and are more enhanced than adjacent normal parotid glands, WTs have mild enhancement in these sequences, which may help in the differentiation between the two tumors [1]. Several studies have investigated the value of DWI in oncocytomas, revealing low ADC values ( $1.06 \pm 0.06 \times 10^{-3} \text{ mm}^2/\text{s}$ ) [6].

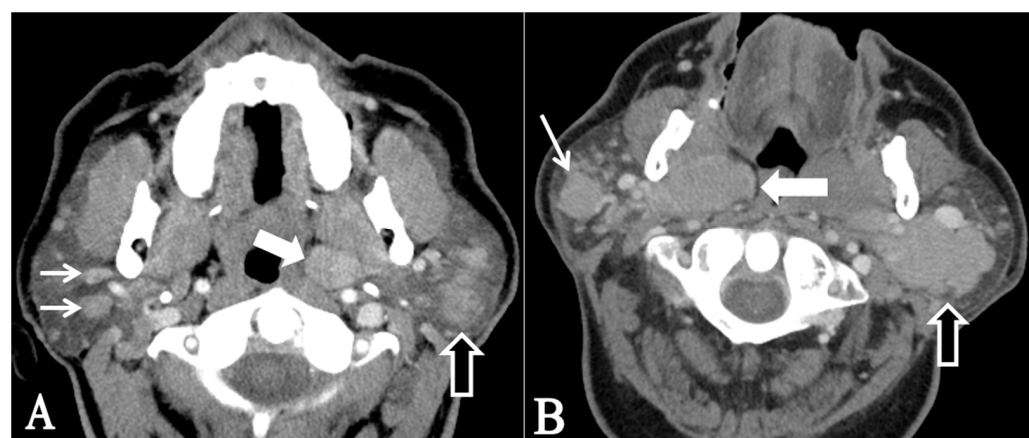


**Figure 5.** Bilateral parotid oncocytomas. Axial contrast-enhanced CT image (A) of bilateral parotid oncocytomas in a 77-year-old male demonstrates an ill-defined heterogeneously enhancing mass within

the posterior portion of the left parotid gland (wide black arrow). Another ovoid mildly enhancing mass is noted within the left parapharyngeal space (wide white arrows). Other smaller multifocal scattered masses are seen within right parotid gland (short narrow arrows). Axial contrast-enhanced CT image (**B**) in a 78-year-old male shows a large dominant lobulated mildly enhancing mass within the left deep parotid gland (wide black arrow). The mass extends into the left parapharyngeal space with mild deformation of its outline. There is an additional large ovoid-shaped mass within the right parotid deep lobe, extending into the right parapharyngeal space (wide white arrow). Other smaller multifocal scattered masses are also seen within parotid glands (long narrow arrows).

### 2.5. Basal Cell Adenoma

Basal cell adenomas (BCAs) are uncommon, comprising around 1–2% of salivary gland neoplasms [27]. They tend to occur in the parotid glands [33]. BCAs share histopathological similarities with adenoid cystic carcinomas (AdCCs) and basal cell adenocarcinomas. The lower number of mitoses, basal layer integrity, slow growth, and lack of vascular or neural invasion suggest its benign nature. Some authors state that BCAs are the benign homologue of AdCCs [33,34].

On CT, BCAs manifest as masses with intratumoral cystic changes, linear bands, and stellate-like non-enhancing components [35]. Cystic BCAs are more frequent. Solid basal cell adenomas typically have a hypointense signal on T2 and restricted diffusion [36]. This is similar to a WT, yet the enhancement pattern can be used to differentiate the entities. Solid portions of BCAs are intensely enhanced on fat-suppressed contrast-enhanced T1 images, whereas WTs are only mildly so [37,38]. Few studies have focused on the role of DWI in depicting the basal adenoma and found mean ADC values of  $1.24 \pm 0.18 \times 10^{-3} \text{ mm}^2/\text{s}$  [7].

### 2.6. Facial Nerve Schwannoma

Facial nerve schwannomas (FNSs) are uncommon benign neoplasms which arise from Schwann cells surrounding the facial (VII) nerve. Schwannomas may arise within the intra-parotid facial nerve, resembling pleomorphic adenomas [39]. The majority of FNSs develop within the intratemporal segments of the facial nerve. FNSs on the extratemporal course of the facial nerve are rare and represent only 9% of cases [40]. These lesions present clinically with unilateral facial palsy, weakness, and/or paralysis. Multiple bilateral schwannomas are usually associated with neurofibromatosis type 2 (NF-2) and schwannomatosis [2].

Intraparotid facial nerve schwannomas present as well-defined round or oval enhancing masses on CT [40]. Typical MR findings include a well-circumscribed mass of an isointense signal on T1 WIs and a hyperintense signal on T2 WIs relative to the muscles, with strong enhancement after gadolinium administration. Larger masses usually have internal cystic degeneration with subsequent heterogeneous enhancement [41].

### 2.7. Benign Lymphoepithelial Lesions

Benign lymphoepithelial lesions (BLELs) are rare and usually found in patients with HIV or Sjögren syndrome [42]. These lesions occur within the 4th-7th decades, with a female predominance, and involve both parotid glands [43]. These lesions typically manifest clinically as painless parotid glands with swelling and enlargement. They have variable presentations, which include cystic and/or mixed solid and cystic masses [2].

The radiologic characteristics of BLELs usually overlap with those of WTs since both frequently present as bilateral cystic and solid parotid masses [44]. CT will differentiate between the cystic components via a thin enhancing rim surrounding the heterogeneously enhancing solid components [45]. The cystic portions of BLELs typically appear with T1 hypointense and T2 hyperintense signals, while the solid portions have variable signal intensity and levels of enhancement [1]. In addition, hypertrophy of Waldeyer's lymphatic ring is strongly associated with BLEL in patients with HIV [46,47].

Other benign parotid gland tumors like myoepithelioma, sebaceous adenoma, cystadenoma, and lymphadenoma are extremely rare and do not have unique imaging characteristics [48].

### 3. Malignant Parotid Tumors

Malignant parotid neoplasms usually present as palpable, very firm, solid masses, often with facial nerve symptoms (Table 1). Typical imaging features of malignant parotid tumors on conventional CT and MRI include an infiltrative mass with ill-defined borders, unclear-unsharp margins and evident invasion of the surrounding structures or perineural invasion [49]. Additionally, most high-grade malignant parotid tumors have a hypointense signal on T2 WIs with heterogeneous enhancement on the post-contrast series [49]. Advanced MR imaging techniques might provide further information to help in the differentiation between benign and malignant parotid tumors [6]. Malignant parotid tumors have restricted diffusion with low ADC [6].

#### 3.1. Mucoepidermoid Carcinomas

Mucoepidermoid carcinomas (MECs) of the parotid gland represent the most common malignant tumors in adults and the pediatric age population [50,51]. They are believed to arise from pluripotent reserve cells of the excretory ducts. MECs have a wide range of histological features owing to their cellular heterogeneity and different cellular compositions: mucinous, intermediate, and epidermoid [52,53]. MECs are classified as high-, intermediate-, or low-grade, correlating with their clinical behavior [50,54].

Low-grade tumors are generally well circumscribed, and the high-grade ones tend to have ill-defined margins with infiltration of the surrounding tissues [54,55]. Intermediate- and high-grade mucoepidermoid carcinomas have a characteristic iso-hypointense signal on T1/T2 WIs reflective of high cellularity. Low-grade tumors tend to have a hyperintense signal on T2 WIs due to their higher content of mucin-secreting cells [55]. High-grade tumors usually show ill-defined margins; however, low-grade MECs can present with similar margins as well, secondary to peri-tumoral inflammatory reaction [55].

MECs can metastasize, with common sites being local lymph nodes and, more distantly, the lung and bone. Perineural tumor invasion is a common feature along the intraparotid facial nerve to its mastoid portion within the temporal bone [2].

#### 3.2. Adenoid Cystic Carcinoma

Adenoid cystic carcinomas (AdCCs) mainly occur in the parotid gland. When they develop within the minor salivary glands, they have a worse prognosis [56–59]. AdCCs represent approximately 1% of all oral and maxillofacial malignant tumors, and 21.9% of all salivary gland malignancies [60]. They often manifest as an infiltrative mass on CT and MRI with a high propensity for perineural spread [61]. AdCCs typically demonstrate a heterogeneous hyperintense signal on T2 WIs with heterogeneous enhancement and unrestricted diffusion on DWI owing to internal cystic changes. Perineural invasion is common and usually appears as ‘skip’ lesions along the course of an apparently normal nerve. Perineural invasion is a major poor prognostic indicator due to the potential risk of extension into the skull base and cranial cavity as well as the high probability of local recurrences, making surgical resection difficult [62].

#### 3.3. Acinic Cell Carcinomas

Acinic cell carcinomas (ACCs) are uncommon salivary gland tumors which occur most often during the 5th–6th decades of life, with a slight female predominance [63].

Ultrasound is the initial imaging modality used to evaluate parotid masses. ACCs typically present as masses with suspicious sonographic criteria [64]. CT is better for evaluating tumor size, involvement, and relationship with surrounding structures, as well as distant metastasis (Figure 6). MRI is the imaging modality of choice for ACC evaluation [56]. ACCs usually appear as masses with a hypointense signal on T1 WIs and T2 WIs, reflecting internal areas of fibrosis, hemosiderin deposition, and calcification. ACCs typically have mild homogeneous enhancement [63]. These tumors typically present with facial nerve perineural spread, manifesting as focal nodular thickening and enhancement

along the course of the nerve. Perineural spread is best captured on contrast-enhanced T1 fat-suppressed images [65,66].



**Figure 6.** Right parotid acinic cell carcinoma in a 61-year-old female. Axial contrast-enhanced CT image demonstrates a large mildly irregular enhancing mass within the posteromedial margin of deep lobe of the right parotid gland (wide arrow).

### 3.4. Salivary Duct Carcinoma

This is an uncommon, and highly aggressive, malignant parotid gland tumor which has a male predilection [67]. Histologically, salivary duct carcinoma resembles mammary ductal carcinoma with an intra-ductal and infiltrating pattern [68]. These tumors are characterized by local recurrence, loco-regional and early distant metastasis, with significant overall mortality [69].

Salivary duct carcinomas do not have any characteristic imaging findings on CT and MRI. Like most aggressive tumors, they present as infiltrative masses with ill-defined margins and frequent internal necrosis [1,70]. Intratumoral calcification is frequently seen in this tumor. Some authors have proposed that a T2 signal could be correlated with the tumor grade, since high-grade tumors tend to have a hypointense signal on T2 WIs [24,71].

### 3.5. Polymorphous Adenocarcinomas

Polymorphous adenocarcinomas (PACs) most commonly occur in the oral cavity and oropharyngeal minor salivary glands [72]. They were previously known as polymorphous low-grade adenocarcinomas prior to the new WHO classification of salivary gland tumors [73]. PACs do not frequently develop de novo or from a pre-existing PA within the major salivary glands [72].

PACs present as indolent slow-growing lesions with an infiltrative growth pattern locally, along with perineural and perivascular invasive characteristics. They have fewer common nodal metastases with rare occurrences of distant spread [74].

The imaging criteria of PACs overlap with those for PAs and AdCCs. PACs typically exhibit irregular walls with heterogeneous enhancement on contrast-enhanced CTs [75]. On MRI, PACs manifest as well-defined masses with T1 intermediate and T2 hyperintense signals as low as  $0.95 \pm 0.09 \times 10^{-3} \text{ mm}^2/\text{s}$  in terms of the ADC. MRI is helpful for the evaluation of the perineural invasion, while CT is crucial in evaluating for bone invasion [76,77].

### 3.6. Primary Squamous Cell Carcinomas

Squamous cell carcinomas (SCCs) are high-grade malignant tumors that account for 0.1–3.4% of all parotid gland tumors [78]. They may be a primary de novo SCC or arise from a pre-existing PA [78,79].

Because these tumors are rare, typical imaging features have not been thoroughly described in the literature. However, their known aggressive behavior and high grade make these tumors appear as ill-defined masses with irregular margins [17]. Infiltration and invasion of the surrounding structures are sometimes seen, with possible perineural invasion [3]. Typical necrotic areas in solid tumors have been described and are best recognized with post-contrast CT imaging and fat-suppressed contrast-enhanced T1 MR images (Figure 7) [78].

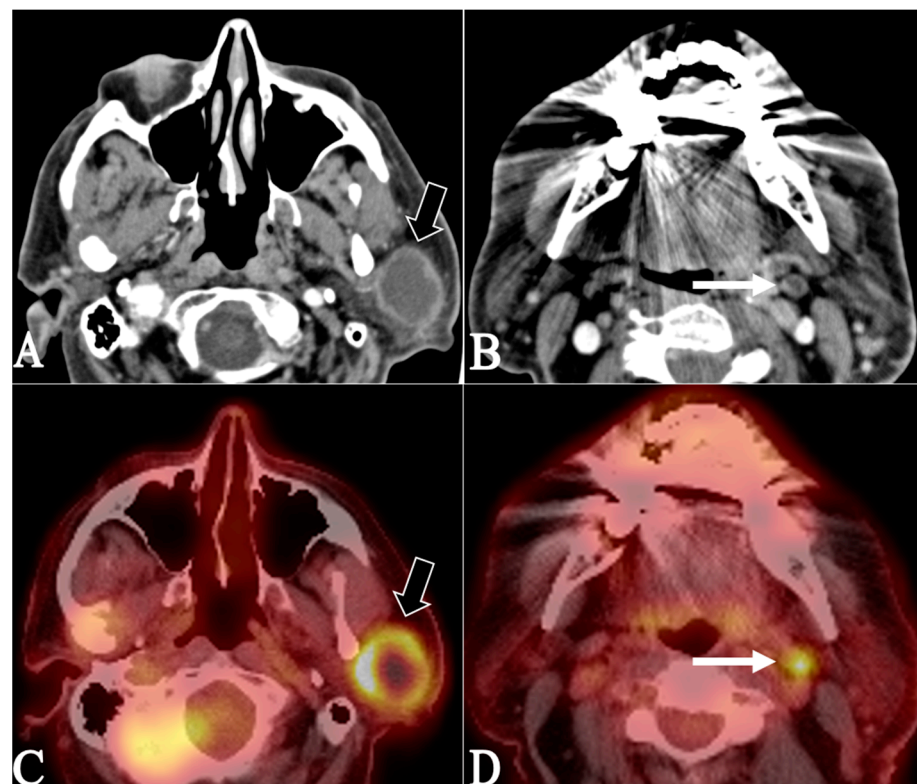


**Figure 7.** Left parotid squamous cell carcinoma in a 77-year-old male. Axial contrast-enhanced CT images (**A,B**) demonstrate a large non uniform peripherally enhancing necrotic mass within the superficial lobe of the left parotid gland (wide arrows). The mass slightly abuts the adjacent mandible without invasion. Small rim-enhancing necrotic left level 2 lymph node is seen (long narrow arrow). Axial FDG-PET/CT images (**C,D**) confirm intense peripheral FDG uptake within the left superficial parotid mass and left level 2 lymph node (wide arrow in image (**C**), and long narrow arrow in image (**D**)).

### 3.7. Metastases

Parotid metastatic lesions should be taken into consideration in patients with a known malignancy presenting with a parotid mass [3]. Dermal and epidermal malignancies of the

scalp and face, like melanoma and squamous cell carcinoma represent the most frequent intraparotid metastatic lesions [80]. Intraparotid metastases from breast or lung cancers are extremely uncommon [81].

The majority (approximately 90%) of intraparotid metastases result from supraclavicular neoplasms through the lymphatic route [54]. They typically present as multifocal masses, however solitary metastatic deposits within the parotid gland have been also described [54,81].

It is hypothesized that intraparotid metastatic deposits are due to propensity of intraparotid lymphatics and lymph nodes, which drain the scalp, external ear, and face [82]. Cutaneous malignancies for instance, squamous cell carcinomas, and melanoma are the most encountered tumors metastasizing to the parotid glands, hence careful clinical examination with high-risk of suspicion should be performed (Figure 8) [82]. The imaging criteria lack significant sensitivity and specificity for intraparotid metastatic disease [51,83]. DWI might help differentiate between benign and malignant lymph nodes through quantitative measurement of ADC [55]. An ADC threshold of  $0.94 \times 10^{-3} \text{ mm}^2/\text{s}$  was suggested by Thoeny et al. with a sensitivity of 84%, and a specificity of 94% [55].

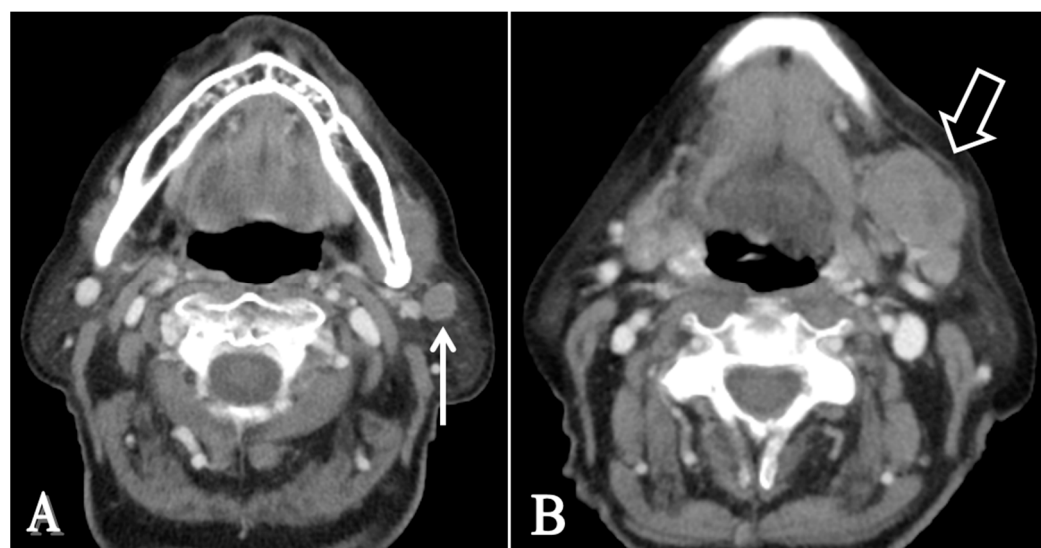


**Figure 8.** Left intraparotid metastatic melanoma in a 75-year-old female. Axial contrast-enhanced CT images (A,B) show a small ovoid-shaped mass within the superficial lobe of the left parotid gland (long white arrow). Note the mass effect and intimate distance to the left retromandibular vein. A large left level 1b metastatic lymph node can be seen in the image (B) (wide black arrow).

### 3.8. Primary Lymphoma

Non-Hodgkin lymphoma (NHL) of the salivary glands is uncommon, accounting for 5% of primary extra-nodal NHLs and 2% of salivary gland neoplasms [84]. The parotid gland is the most frequently involved salivary gland and the site of about 75% of these cases [84]. Extra-nodal marginal zone B-cell lymphoma (MZL) of the mucosa-associated lymphoid tissue (MALT) type, diffuse large B-cell lymphoma, and follicular B-cell lymphoma are the most commonly encountered NHL subtypes within parotid glands [85].

Primary parotid lymphomas have variable presentations, ranging from focal solid or solid–cystic masses to diffusely solid–cystic changes in the gland and multiple solid masses [84,86]. The parotid gland is the most commonly involved salivary gland in secondary lymphoma, being seen in approximately 80% of cases. Patients with Sjogren's syndrome have a 44-times-greater risk of developing NHL compared with the general population [87]. CT and MRI are equally effective for the evaluation of tumor characteristics, yet CT is preferred due to its accessibility, lower cost, and fast results (Figure 9) [87].  $^{18}\text{F}$ -FDG-PET/CT evaluation is essential for proper staging [88].



**Figure 9.** Right parotid lymphoma in a 60-year-old female. Axial contrast-enhanced CT image demonstrates a large micro-lobulated mildly enhancing mass involving most of the posterior right parotid gland (wide arrow). The lesion extends into subcutaneous fat with skin infiltration (short white arrows).

#### 4. Conclusions

Preoperative imaging evaluation of the parotid gland tumors is imperative to differentiate between benign and malignant neoplasms and decrease the rate of unnecessary interventional procedures. Multimodality imaging with CT and various MR sequences are usually required to suggest a diagnosis. Figure 10 shows a suggested approach for the evaluation of parotid masses with the proper imaging modality and the impact of preoperative imaging on management planning.

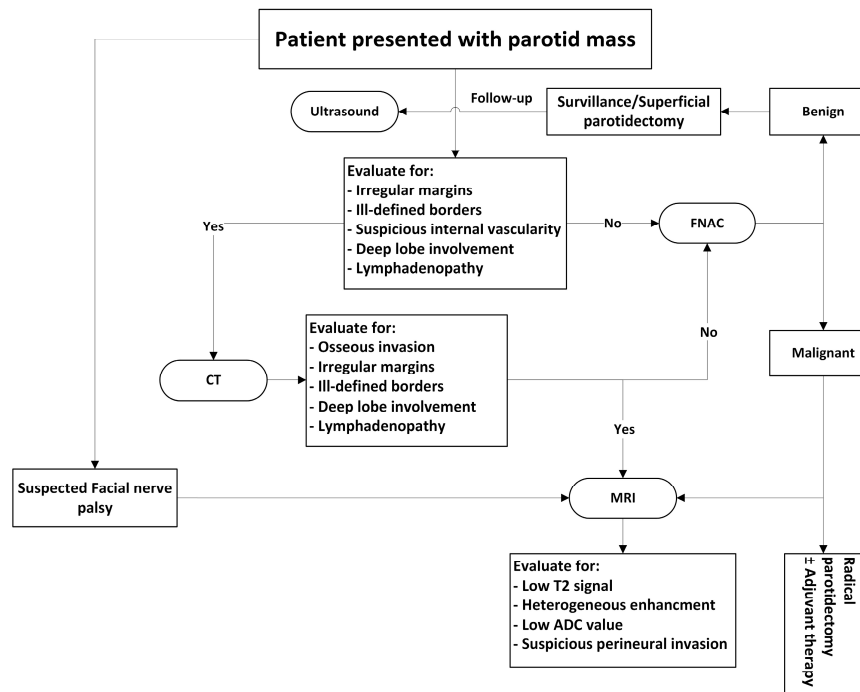


**Figure 10.** Expected impact of preoperative imaging on management of clinically presented parotid masses. ADC: apparent diffusion coefficient; CT: computed tomography; FNAC: fine-needle aspiration cytology; MRI: magnetic resonance imaging.

**Author Contributions:** Conceptualization, A.N., E.M. (Esmat Mahmoud) and C.L.-S.; methodology, A.N.; software, A.N.; validation, A.N., E.M. (Eman Mahdi) and C.L.-S.; formal analysis, A.N.; investigation, E.M. (Esmat Mahmoud); resources, E.M. (Eman Mahdi); data curation, H.A.; writing—original draft preparation, A.N.; writing—review and editing, E.M. (Eman Mahdi), J.P.C., C.L.-S. and A.N.; visualization, E.M. (Eman Mahdi) and A.N.; supervision, A.N. All authors have read and agreed to the published version of the manuscript.

**Funding:** This research received no external funding.

**Institutional Review Board Statement:** This study was conducted in accordance with the Declaration of Helsinki and approved by the Institutional Review Board of University of Missouri (protocol code 375231 and date of approval 11 April 2022).

**Informed Consent Statement:** Patient consent was waived due to the study design as a review article.

**Data Availability Statement:** Data are available upon request.

**Conflicts of Interest:** The authors declare no conflicts of interest.

## References

1. Tartaglione, T.; Botto, A.; Sciandra, M.; Gaudino, S.; Danieli, L.; Parrilla, C.; Paludetti, G.; Colosimo, C. Differential diagnosis of parotid gland tumours: Which magnetic resonance findings should be taken in account? *Acta Otorhinolaryngol. Ital.* **2015**, *35*, 314–320. [CrossRef] [PubMed]
2. Teh, A.; Kumar, A.; Teh, C.; II, O.; Alhilali, L. Overview of Parotid Gland Masses. *J. Am. Osteopath Coll. Radiol.* **2018**, *7*, 5–10.
3. Thielker, J.; Grosheva, M.; Ihrler, S.; Wittig, A.; Guntinas-Lichius, O. Contemporary Management of Benign and Malignant Parotid Tumors. *Front. Surg.* **2018**, *5*, 39–56. [CrossRef] [PubMed]
4. Bussu, F.; Parrilla, C.; Rizzo, D.; Almadori, G.; Paludetti, G.; Galli, J. Clinical approach and treatment of benign and malignant parotid masses, personal experience. *Acta Otorhinolaryngol. Ital.* **2011**, *31*, 135–143.
5. Christe, A.; Waldherr, C.; Hallett, R.; Zbaeren, P.; Thoeny, H. MR imaging of parotid tumors: Typical lesion characteristics in MR imaging improve discrimination between benign and malignant disease. *AJR Am. J. Neuroradiol.* **2011**, *32*, 1202–1207. [CrossRef]
6. Gökçe, E. Multiparametric Magnetic Resonance Imaging for the Diagnosis and Differential Diagnosis of Parotid Gland Tumors. *J. Magn. Reason. Imaging* **2020**, *52*, 11–32. [CrossRef]
7. Abdel Razek, A.A.K. Routine and Advanced Diffusion Imaging Modules of the Salivary Glands. *Neuroimaging Clin. N. Am.* **2018**, *28*, 245–254. [CrossRef]
8. Bokhari, M.R.; Greene, J. *Pleomorphic Adenoma; StatPearls*; Treasure Island, FL, USA, 2020. Available online: <https://www.ncbi.nlm.nih.gov/books/NBK430829/> (accessed on 5 March 2019).
9. Dulguerov, P.; Todic, J.; Pusztaszeri, M.; Alotaibi, N.H. Why Do Parotid Pleomorphic Adenomas Recur? A Systematic Review of Pathological and Surgical Variables. *Front. Surg.* **2017**, *4*, 26–34. [CrossRef]
10. Shishegar, M.; Ashraf, M.J.; Azarpira, N.; Khademi, B.; Hashemi, B.; Ashrafi, A. Salivary gland tumors in maxillofacial region: A retrospective study of 130 cases in a southern Iranian population. *Pathol. Res. Int.* **2011**, *2011*, 9343–9350. [CrossRef]
11. Farhat, F.; Asnir, R.A.; Yudhistira, A.; Daulay, E.R.; Sagala, I.P. An Uncommon Occurrence of Pleomorphic Adenoma in the Submandibular Salivary Gland: A Case Report. *Open Access Maced. J. Med. Sci.* **2018**, *6*, 1101–1103. [CrossRef]
12. Terra, G.T.C.; Oliveira, J.X.D.; Hernandez, A.; Lourenço, S.V.; Arita, E.S.; Cortes, A.R.G. Diffusion-weighted MRI for differentiation between sialadenitis and pleomorphic adenoma. *Dentomaxillofac Radiol.* **2017**, *46*, 20160257. [CrossRef] [PubMed]
13. Nada, A.; Youssef, A.; El Basmy, A.; Amin, A.; Shokry, A. Diffusion-Weighted Imaging of the Parotid Gland: Can the Apparent Diffusion Coefficient Discriminate Between Normal and Abnormal Parotid Gland Tissues? *J. Clin. Pr. Res.* **2017**, *39*, 125–130. [CrossRef]
14. Nada, A.; Hady, D.; Youssef, A.; Mahmoud, E.; Assad, R.E. Accuracy of combined quantitative diffusion-weighted MRI and routine contrast-enhanced MRI in discrimination of benign and malignant salivary gland tumors. *Neuroradiol. J.* **2020**, *33*, 216–223. [CrossRef] [PubMed]
15. McGarry, J.G.; Redmond, M.; Tuffy, J.B.; Wilson, L.; Looby, S. Metastatic pleomorphic adenoma to the supraspinatus muscle: A case report and review of a rare aggressive clinical entity. *J. Radiol. Case Rep.* **2015**, *9*, 1–8. [CrossRef] [PubMed]
16. Kanatasa, A.; Hoa, M.W.S.; Mücke, T. Current thinking about the management of recurrent pleomorphic adenoma of the parotid: A structured review. *Br. J. Oral Maxillofac. Surg. May* **2018**, *56*, 243–248. [CrossRef]
17. Bahrami, A.; Dalton, J.D.; Bangalore, S.; Henry, C.; Krane, J.F.; Navid, F.; Ellison, D.W. Disseminated carcinoma ex pleomorphic adenoma in an adolescent confirmed by application of PLAG1 immunohistochemistry and FISH for PLAG1 rearrangement. *Head Neck Pathol.* **2012**, *6*, 377–383. [CrossRef]
18. Rzepakowska, A.; Osuch-Wójcikiewicz, E.; Sobol, M.; Cruz, R.; Sielska-Badurek, E.; Niemczyk, K. The differential diagnosis of parotid gland tumors with high-resolution ultrasound in otolaryngological practice. *Eur. Arch. Otorhinolaryngol.* **2017**, *274*, 3231–3240. [CrossRef]
19. Gary, L.E.; Paul, L.A. *Modern Surgical Pathology*, 2nd ed.; Elsevier Health Sciences: Amsterdam, The Netherlands, 2009.

20. Yu, C.; Song, Z.; Xiao, Z.; Lin, Q.; Dong, X. Mucoepidermoid carcinoma arising in Warthin's tumor of the parotid gland: Clinicopathological characteristics and immunophenotypes. *Sci. Rep.* **2016**, *6*, 149–157. [[CrossRef](#)]
21. Ferreira, J.A.S.; Pio, R.B.; Takano, G.H.S.; Miziara, H.L.; Nascimento, L.A. Synchronous bilateral Warthin tumors: A case report. *Int. Arch. Otorhinolaryngol.* **2014**, *18*, 217–220. [[CrossRef](#)]
22. Nicolai, G.; Ventucci, E.; Antonucci, P.; Costantino, V.; Brunelli, G.; Mariani, G.; Saltarel, A.; Lorè, B.; Calabrese, L. Bilateral and multifocal Warthin's tumor of parotid gland: Two case reports and review of literature. *Oral Implantol.* **2014**, *7*, 25–31.
23. Kessler, A.T.; Bhatt, A.A. Review of the Major and Minor Salivary Glands, Part 2: Neoplasms and Tumor-like Lesions. *J. Clin. Imaging Sci.* **2018**, *8*, 48–57. [[CrossRef](#)] [[PubMed](#)]
24. Chowdhury, R.M.; Roy, D.; Pattari, S.K. Lipoma of parotid: A case report. *Egypt. J. Otolaryngol.* **2017**, *33*, 691–693. [[CrossRef](#)]
25. Paparo, F.; Massarelli, M.; Giuliani, G. A rare case of parotid gland lipoma arising from the deep lobe of the parotid gland. *Ann. Maxillofac. Surg.* **2016**, *6*, 308–310. [[CrossRef](#)] [[PubMed](#)]
26. Zhang, J.; Li, Y.; Zhao, Y.; Qiao, J. CT and MRI of superficial solid tumors. *Quant. Imaging Med. Surg.* **2018**, *8*, 232–251. [[CrossRef](#)] [[PubMed](#)]
27. Watanabe, T.; Yoshida, Y.; Yamamoto, O. Oncocytoma of the parotid gland presenting as a subcutaneous tumor. *Eur. J. Dermatol.* **2011**, *21*, 273–274.
28. El Korbi, A.; Jellali, S.; Njima, M.; Harrathi, K.; Bouatay, R.; Ferjaoui, M.; Kolsi, N.; Koubaa, J. Parotid Gland Oncocytoma: A Rare Case and Literature Review. *J. Med. Cases* **2019**, *10*, 146–149. [[CrossRef](#)]
29. Tan, T.J.; Tan, T.Y. CT Features of Parotid Gland Oncocytomas: A Study of 10 Cases and Literature Review. *Am. J. Neuroradiol.* **2010**, *31*, 1413–1417. [[CrossRef](#)]
30. Patel, N.D.; Van Zante, A.; Eisele, D.W.; Harnsberger, H.R.; Glastonbury, C.M. Oncocytoma: The Vanishing Parotid Mass. *Am. J. Neuroradiol.* **2011**, *32*, 1703–1706. [[CrossRef](#)]
31. Sepúlveda, I.; Platín, E.; Spencer, M.L.; Mucientes, P.; Frelinghuysen, M.; Ortega, P.; Ulloa, D. Oncocytoma of the Parotid Gland: A Case Report and Review of the Literature. *Case Rep. Oncol.* **2014**, *7*, 109–116. [[CrossRef](#)]
32. Matsusue, E.; Fujihara, Y.; Matsuda, E.; Tokuyasu, Y.; Nakamoto, S.; Nakamura, K.; Ogawa, T. Vanishing Parotid Tumors on MR Imaging. *Yonago Acta Med.* **2018**, *61*, 33–39. [[CrossRef](#)]
33. Chung, W.Y.; Kim, C.H. Basal cell adenoma in the deep portion of the parotid gland: A case report. *J. Korean Assoc. Oral Maxillofac. Surg.* **2015**, *41*, 352–356. [[CrossRef](#)] [[PubMed](#)]
34. Kanaujia, S.K.; Singh, A.; Nautiyal, S.; Ashutosh, K. Basal Cell Adenoma of Parotid Gland: Case Report and Review of Literature. *Indian J. Otolaryngol. Head Neck Surg.* **2015**, *67*, 430–433. [[CrossRef](#)] [[PubMed](#)]
35. Kanaujia, S.K.; Singh, A.; Nautiyal, S.; Ashutosh, K. Basal cell adenoma of the parotid gland; MR features and differentiation from pleomorphic adenoma. *Dentomaxillofac Radiol.* **2016**, *45*, 322–329.
36. Ming-Wei, X.; Zi-Liang, C.; Hai-Yan, W.; Guang-Zi, S.; Hui-Jun, H.; Zhi-Long, Y.; Wan-Shao, L.; Zhuo, W. MR Imaging Features of Basal Cell Adenoma of the Parotid Gland: Differentiation from Pleomorphic Adenoma and Warthin Tumor. *Int. J. Radiol. Imaging Technol.* **2018**, *4*, 33–40. [[CrossRef](#)]
37. El Shahat, H.M.; Fahmy, H.S.; Gouhar, G.K. Diagnostic value of gadolinium-enhanced dynamic MR imaging for parotid gland tumors. *Egypt. J. Radiol. Nucl. Med.* **2013**, *44*, 203–207. [[CrossRef](#)]
38. Seo, B.F.; Choi, H.J.; Seo, K.J.; Jung, S.-N. Intraparotid facial nerve schwannomas. *Arch. Craniofac Surg.* **2019**, *20*, 71–74. [[CrossRef](#)]
39. Jaiswal, A.; Mridha, A.R.; Nath, D.; Bhalla, A.S.; Thakkar, A. Intraparotid facial nerve schwannoma: A case report. *World J. Clin. Cases* **2015**, *3*, 322–326. [[CrossRef](#)]
40. Damar, M.; Dinç, A.E.; Şevik Eliçora, S.; Bişkin, S.; Erten, G.; Biz, S. Facial nerve schwannoma of parotid gland: Difficulties in diagnosis and management. *Case Rep. Otolaryngol.* **2016**, *2016*, 3939685. [[CrossRef](#)]
41. Arutyunyan, S.; Matthew, U. Benign Lymphoepithelial Lesion of the Parotid Gland in the Setting of HAART. *J. Int. Assoc. Provid. AIDS Care* **2017**, *16*, 120–124. [[CrossRef](#)]
42. Sandhu, V.K.; Sharma, U.; Singh, N.; Puri, A. Cytological spectrum of salivary gland lesions and their correlation with epidemiological parameters. *J. Oral Maxillofac. Pathol.* **2017**, *21*, 203–210. [[CrossRef](#)]
43. Rimmer, R.A.; Cottrill, E.E. Multifocal Warthin's Tumor: An Uncommon Presentation of Bilateral Cervical Lymphadenopathy. *Case Rep. Otolaryngol.* **2018**, *3*, 791–825. [[CrossRef](#)] [[PubMed](#)]
44. Alexander, A.; Hunter, K.; Wasdahl, D.; Markovic, M. Lymphoepithelial cyst as a herald of HIV seropositivity in a patient with known history of neurocysticercosis and suspected parotid cysticercosis. *BJR | Case Rep.* **2016**, *2*, 119–123. [[CrossRef](#)] [[PubMed](#)]
45. Joshi, J.; Shah, S.; Agarwal, D.; Khasgiwal, A. Benign lymphoepithelial cyst of parotid gland: Review and case report. *J. Oral Maxillofac. Pathol.* **2018**, *22*, S91–S97. [[PubMed](#)]
46. Abdullah, A.; Rivas, F.R.; Srinivasan, A. Imaging of the salivary glands. *Semin Roentgenol.* **2013**, *48*, 65–74. [[CrossRef](#)] [[PubMed](#)]
47. Yerli, H.; Aydin, E.; Haberal, N.; Harman, A.; Kaskati, T.; Alibek, S. Diagnosing common parotid tumors with magnetic resonance imaging including diffusion-weighted imaging vs. fine-needle aspiration cytology: A comparative study. *Dentomaxillofac Radiol.* **2010**, *39*, 349–355. [[CrossRef](#)]
48. Bakst, R.L.; Glastonbury, C.M.; Parvathaneni, U.; Katabi, N.; Hu, K.S.; Yom, S.S. Perineural Invasion and Perineural Tumor Spread in Head and Neck Cancer. *Radiat. Oncol. Biol.* **2019**, *103*, 1109–1124. [[CrossRef](#)] [[PubMed](#)]
49. Xu, Z.; Zheng, S.; Pan, A.; Cheng, X.; Gao, M. A multiparametric analysis based on DCE-MRI to improve the accuracy of parotid tumor discrimination. *Eur. J. Nucl. Med. Mol. Imaging* **2019**, *46*, 2228–2234. [[CrossRef](#)]

50. Joseph, T.P.; Joseph, C.P.; Jayalakshmy, P.; Poothiode, U. Diagnostic challenges in cytology of mucoepidermoid carcinoma: Report of 6 cases with histopathological correlation. *J. Cytol.* **2015**, *32*, 21–24. [[CrossRef](#)]
51. Kashiwagi, N.; Murakami, T.; Toguchi, M.; Nakanishi, K.; Hidaka, S.; Fukui, H.; Kimura, M.; Kitano, M.; Tomiyama, N. Metastases to the parotid nodes: CT and MR imaging findings. *Dentomaxillofac Radiol.* **2016**, *45*, 201–206. [[CrossRef](#)]
52. Kim, J.; Kim, E.; Park, C.S.; Choi, Y.; Kim, Y.H.; Choi, E.C. Characteristic sonographic findings of Warthin's tumor in the parotid gland. *J. Clin. Ultrasound* **2004**, *32*, 78–81. [[CrossRef](#)]
53. Iro, H.; Zenk, J. Salivary gland diseases in children. *GMS Curr. Top Otorhinolaryngol. Head Neck Surg.* **2014**, *13*, Doc06. [[PubMed](#)]
54. Koeller, K.K. Radiologic Features of Sinonasal Tumors. *Head Neck Pathol.* **2016**, *10*, 1–12. [[CrossRef](#)] [[PubMed](#)]
55. Diwakar, J.K.; Agarwal, A.; Garg, C.; Giri, K.; Dandriyal, R.; Kumar, G. A Rare Case of Mucoepidermoid Carcinoma of Parotid with Mandibular Metastasis. *Ann. Maxillofac. Surg.* **2019**, *9*, 205–207. [[CrossRef](#)] [[PubMed](#)]
56. Coca-Pelaz, A.; Rodrigo, J.P.; Bradley, P.J.; Poorten, V.V.; Triantafyllou, A.; Hunt, J.L.; Strojan, P.; Rinaldo, A.; Haigentz, M.; Takes, R.P.; et al. Adenoid cystic carcinoma of the head and neck: An update. *Oral Oncol.* **2015**, *51*, 652–661. [[CrossRef](#)] [[PubMed](#)]
57. Godge, P.; Sharma, S.; Yadav, M. Adenoid cystic carcinoma of the parotid gland. *Contemp. Clin. Dent.* **2012**, *3*, 223–226. [[CrossRef](#)]
58. Lin, H.H.; Limesand, K.H.; Ann, D.K. Current State of Knowledge on Salivary Gland Cancers. *Crit. Rev. Oncog.* **2018**, *23*, 139–151. [[CrossRef](#)]
59. Pinakapani, R.; Nallan, C.S.K.; Reddy, L.; Yarram, S.; Boringi, M.; Waghray, S. Adenoid Cystic Carcinoma of the Head and Neck—literature review. *Qual. Prim. Care* **2015**, *23*, 309–314.
60. Sepúlveda, I.; Frelinghuysen, M.; Platin, E.; Spencer, M.L.; Urra, A.; Ortega, P. Acinic cell carcinoma of the parotid gland: A case report and review of the literature. *Case Rep. Oncol.* **2015**, *8*, 1–8. [[CrossRef](#)]
61. Khalife, A.; Bakhshaee, M.; Davachi, B.; Mashhad, L.; Khazaeni, K. The Diagnostic Value of B-Mode Sonography in Differentiation of Malignant and Benign Tumors of the Parotid Gland. *Iran. J. Otorhinolaryngol.* **2016**, *28*, 305–312.
62. Amit, M.; Eran, A.; Billan, S.; Fridman, E.; Na'Ara, S.; Charas, T.; Gil, Z. Perineural Spread in Noncutaneous Head and Neck Cancer: New Insights into an Old Problem. *J. Neurol. Surg. B Skull Base* **2016**, *77*, 86–95. [[CrossRef](#)]
63. Frunza, A.; Slavescu, D.; Lascar, I. Perineural invasion in head and neck cancers—A review. *J. Med. Life* **2014**, *7*, 121–123. [[PubMed](#)]
64. Weon, Y.C.; Park, S.-W.; Kim, H.-J.; Jeong, H.-S.; Ko, Y.-H.; Park, I.S.; Kim, S.T.; Baek, C.H.; Son, Y.-I. Salivary duct carcinomas: Clinical and CT and MR imaging features in 20 patients. *Neuroradiology* **2012**, *54*, 631–640. [[CrossRef](#)] [[PubMed](#)]
65. Acharya, S.; Padmini, S.; Koneru, A.; Krishnapillai, R. Intraoral salivary duct carcinoma: A case report and a brief review. *J. Oral. Maxillofac. Pathol.* **2014**, *18*, S121–S127. [[CrossRef](#)]
66. Wang, X.; Luo, Y.; Li, M.; Yan, H.; Sun, M.; Fan, T. Management of salivary gland carcinomas—A review. *Oncotarget* **2017**, *8*, 3946–3956. [[CrossRef](#)] [[PubMed](#)]
67. Cicero, G.; D'angelo, T.; Racchiusa, S.; Salamone, I.; Visalli, C.; Bottari, A.; Blandino, A.; Mazziotti, S. Cross-sectional Imaging of Parotid Gland Nodules: A Brief Practical Guide. *J. Clin. Imaging Sci.* **2018**, *8*, 14–22. [[CrossRef](#)] [[PubMed](#)]
68. Mlika, M.; Kourda, N.; Zidi, Y.; Aloui, R.; Zneidi, N.; Rammeh, S.; Zermani, R.; Jilani, S. Salivary duct carcinoma of the parotid gland. *J. Oral Maxillofac. Pathol.* **2012**, *16*, 134–136. [[CrossRef](#)] [[PubMed](#)]
69. Khosla, D.; Verma, S.; Gupta, N.; Punia, R.S.; Kaur, G.; Pandey, A.K.; Dimri, K. Polymorphous low-grade adenocarcinoma of the parotid in a teenager. *Iran. J. Otorhinolaryngol.* **2017**, *29*, 299–302. [[PubMed](#)]
70. Guda, S.; Kalapannavar, A.N.; Kumar, K.P.M.; Lakshmi, S.S. Polymorphous low-grade adenocarcinoma of parotid gland—A case report and review. *J. Med. Radiol. Pathol. Surg.* **2018**, *5*, 21–23. [[CrossRef](#)]
71. Takahashi, H.; Kashiwagi, N.; Chikugo, T.; Nakanishi, K.; Tomita, Y.; Murakami, T. Squamous cell carcinoma originating in the parotid gland: MRI features with histopathological correlation. *Clin. Radiol.* **2014**, *69*, 41–44. [[CrossRef](#)] [[PubMed](#)]
72. Keerthi, R.; Raut, R.P.; Vaibhav, N.; Ghosh, A. Carcinoma ex pleomorphic adenoma: Diagnostic dilemma and treatment protocol. *Indian J. Dent.* **2014**, *5*, 157–160.
73. Żurek, M.; Fus, Ł.; Niemczyk, K.; Rzepakowska, A. Salivary gland pathologies: Evolution in classification and association with unique genetic alterations. *Eur. Arch. Otorhinolaryngol.* **2023**, *280*, 4739–4750. [[CrossRef](#)]
74. Antony, J.; Gopalan, V.; Smith, R.A.; Lam, A.K.Y. Carcinoma ex pleomorphic adenoma: A comprehensive review of clinical, pathological and molecular data. *Head Neck Pathol.* **2012**, *6*, 1–9. [[CrossRef](#)]
75. Hiyama, T.; Kuno, H.; Sekiya, K.; Oda, S.; Kobayashi, T. Imaging of malignant minor salivary gland tumors of the head and neck. *Radiographics* **2021**, *41*, 175–191. [[CrossRef](#)] [[PubMed](#)]
76. Gökçe, E.; Beyhan, M. Advanced magnetic resonance imaging findings in salivary gland tumors. *World J. Radiol.* **2022**, *14*, 256–271. [[CrossRef](#)] [[PubMed](#)]
77. Zheng, N.; Li, R.; Liu, W.; Shao, S.; Jiang, S. The diagnostic value of combining conventional, diffusion-weighted imaging and dynamic contrast-enhanced MRI for salivary gland tumors. *Br. J. Radiol.* **2018**, *91*, 20170707. [[CrossRef](#)] [[PubMed](#)]
78. Franzen, A.; Buchali, A.; Lieder, A. The rising incidence of parotid metastases: Our experience from four decades of parotid gland surgery. *Acta Otorhinolaryngol. Ital.* **2017**, *37*, 264–269. [[CrossRef](#)] [[PubMed](#)]
79. Cao, X.S.; Cong, B.B.; Yu, Z.Y. Parotid gland metastasis from carcinoma of the breast detected by PET/CT: Case report and review. *Medicine* **2018**, *97*, 106–116. [[CrossRef](#)] [[PubMed](#)]
80. Thoeny, H.C. Imaging of salivary gland tumours. *Cancer Imaging* **2007**, *7*, 52–62. [[CrossRef](#)]
81. Kılıçkaya, M.M.; Aynali, G.; Ceyhan, A.M.; Çırış, M. Metastatic Malignant Melanoma of Parotid Gland with a Regressed Primary Tumor. *Case Rep. Otolaryngol.* **2016**, *2016*, 1–4. [[CrossRef](#)]

82. Zhu, L.; Wang, P.; Yang, J.; Yu, Q. Non-Hodgkin lymphoma involving the parotid gland: CT and MR imaging findings. *Dentomaxillofac Radiol.* **2013**, *42*, 46–54. [[CrossRef](#)]
83. Kim, H.J.; Yoon, D.Y.; Hong, J.H.; Yun, E.J.; Baek, S.; Kim, E.S.; Park, M.W.; Kwon, K.H. Intra-parotid lymph node metastasis in patients with non-cutaneous head and neck cancers: Clinical and imaging features for differentiation from simultaneous parotid primary tumor. *Acta Radiol.* **2020**, *61*, 1628–1635. [[CrossRef](#)] [[PubMed](#)]
84. Gilbert, M.R.; Sharma, A.; Schmitt, N.C.; Johnson, J.T.; Ferris, R.L.; Duvvuri, U.; Kim, S. A 20-Year Review of 75 Cases of Salivary Duct Carcinoma. *JAMA Otolaryngol. Head Neck Surg.* **2016**, *142*, 489–495. [[CrossRef](#)] [[PubMed](#)]
85. Lee, H.G.; Lee, J.Y.; Song, J.M. Malignant lymphoma on parotid gland: A clinical case. *J. Korean Assoc. Oral Maxillofac. Surg.* **2017**, *43*, 138–143. [[CrossRef](#)] [[PubMed](#)]
86. Mahmoud, E.M.; Howard, E.; Ahsan, H.; Cousins, J.P.; Nada, A. Cross-sectional imaging evaluation of atypical and uncommon extra-nodal head and neck Non-Hodgkin lymphoma: Case series. *J. Clin. Imaging Sci.* **2023**, *13*, 6. [[CrossRef](#)]
87. Alunno, A.; Leone, M.C.; Giacomelli, R.; Carubbi, F. Lymphoma and Lymphomagenesis in Primary Sjögren's Syndrome. *Front. Med.* **2018**, *13*, 102–109. [[CrossRef](#)]
88. Ren, Y.; Huang, L.; Han, Y.; Cui, Z.; Li, J.; Dong, C.; Liu, J. 18F-FDG PET/CT for staging and response assessment of primary parotid MALT lymphoma with multiple sites involvement: A case report. *Medicine* **2019**, *98*, 270–278. [[CrossRef](#)]

**Disclaimer/Publisher's Note:** The statements, opinions and data contained in all publications are solely those of the individual author(s) and contributor(s) and not of MDPI and/or the editor(s). MDPI and/or the editor(s) disclaim responsibility for any injury to people or property resulting from any ideas, methods, instructions or products referred to in the content.